ARTICLE

Semimechanistic modeling of copeptin and aldosterone kinetics and dynamics in response to rehydration treatment for diabetic ketoacidosis in children

Marije E. Otto[1,2] | **Marie-Anne Burckhardt**[3,4] | **Gabor Szinnai**[3,4] | **Marc Pfister**[1,5] | **Verena Gotta**[1]

[1]Pediatric Pharmacology and Pharmacometrics, University Children's Hospital Basel, University of Basel, Basel, Switzerland

[2]Leiden Academic Centre for Drug Research, Leiden University, Leiden, The Netherlands

[3]Pediatric Endocrinology and Diabetology, University Children's Hospital Basel, University of Basel, Basel, Switzerland

[4]Department of Clinical Research, University Hospital Basel, University of Basel, Basel, Switzerland

[5]Certara, Princeton, New Jersey, USA

Correspondence
Marije E. Otto, Leuvenstraat 38, 2313XZ Leiden, The Netherlands.
Email: marije_otto@live.nl

Abstract

Diabetic ketoacidosis (DKA), a frequent complication of type 1 diabetes (T1D), is characterized by hyperosmolar hypovolemia. The response of water-regulating hormones arginine vasopressin (AVP; antidiuretic hormone) and aldosterone to DKA treatment in children is not well understood, although they may have potential as future diagnostic, prognostic, and/or treatment monitoring markers in diabetic patients. We aimed to characterize the dynamics of the response in copeptin (marker for AVP) and aldosterone secretion to rehydration treatment in pediatric patients with DKA. Data originated from a prospective, observational, multicenter study including 28 pediatric T1D patients treated for DKA (median age, 11.5 years; weight, 35 kg). Serial measurements of hormone levels were obtained during 72 h following rehydration start. Semimechanistic pharmacometric modeling was used to analyze the kinetic/dynamic relationship of copeptin and aldosterone secretion in response to the correction of hyperosmolality and hypovolemia, respectively. Modeling revealed different sensitivities for osmolality-dependent copeptin secretion during the first 72 h of rehydration, possibly explained by an osmotic shift introduced by hypovolemia. Response in aldosterone secretion to the correction of hypovolemia seemed to be delayed, which was well described by an extra upstream turnover compartment, possibly representing chronic upregulation of aldosterone synthase (cytochrome P450 11B2). In conclusion, semimechanistic modeling provided novel physiological insights in hormonal water regulation in pediatric patients during DKA treatment, providing rationale to further evaluate the potential of monitoring copeptin, but not aldosterone due to its delayed response, for future optimization of rehydration treatment to reduce the risk of acute complications such as cerebral edema.

Study Highlights

WHAT IS THE CURRENT KNOWLEDGE ON THE TOPIC?
Water-regulating hormones arginine vasopressin (AVP) and aldosterone are highly elevated in children with type 1 diabetes (T1D) treated for diabetic ketoacidosis (DKA).

WHAT QUESTION DID THIS STUDY ADDRESS?
How do the changes in copeptin (as surrogate marker for AVP) and aldosterone levels in children with T1D relate to the changes in osmolality and dehydration during rehydration treatment?

WHAT DOES THIS STUDY ADD TO OUR KNOWLEDGE?
Developed semimechanistic turnover models provided novel physiologic insights into hormonal regulation during rehydration for DKA. Secretion dynamics of copeptin in response to serum osmolality changes were found to vary with rehydration status, possibly indicating an osmotic shift after full rehydration. Prolonged aldosterone secretion during the correction of fluid deficit suggests regulation by an upstream signal with slow turnover, potentially representing upregulated cytochrome P450 11B2 expression.

HOW MIGHT THIS CHANGE DRUG DISCOVERY, DEVELOPMENT, AND/OR THERAPEUTICS?
Copeptin (fast response), but not aldosterone (delayed response), may be further evaluated as marker for DKA rehydration protocol optimization, for example, to decrease the risk of cerebral edema. The suggested chronic upregulation of aldosterone deserves further investigation, as it is also associated with cardiovascular risk and insulin resistance in other populations.

INTRODUCTION

Diabetic ketoacidosis (DKA) is a frequent and potentially life-threatening complication in children with type 1 diabetes mellitus (T1D), especially in younger, undiagnosed patients.[1] Hyperglycemia and hyperketonemia, caused by insulin deficiency, induce osmotic diuresis, contributing to dehydration and the development of a hypovolemic hyperosmolar state.[1–3] DKA is treated with fluid and electrolyte replacement combined with insulin therapy. DKA is the main cause of diabetes-related deaths in patients diagnosed with T1D and has a mortality rate of 0.16%–0.25%.[4–6] Occurrence of cerebral edema during DKA treatment is a possible complication, which might be associated with the rate of fluid administration.[7–9] A better understanding of the hormonal regulation of water homeostasis in children with DKA is crucial, as it may provide a basis to develop personalized monitoring and treatment strategies and reduce the risk of complications.

It has been reported that levels of the major water- and salt-regulating hormones arginine vasopressin (AVP; antidiuretic hormone) and aldosterone are increased during DKA.[10,11] AVP secretion is thought to be induced mainly in response to hyperosmolality and increases renal water reabsorption.[12–14] Measuring AVP directly is difficult due to stability problems, therefore copeptin, a peptide derived from the precursor protein of AVP, can be measured as a substitute.[15] It has also been found to respond to stress (myocardial infarction, ischemic stroke, sepsis)[16–21] and is being investigated as a potential diagnostic, prognostic, and disease-monitoring marker in various conditions, including T1D.[20,22–26] Aldosterone is part of the renin-angiotensin-aldosterone system (RAAS)[27] and is secreted in response to angiotensin II, which is stimulated by renin in response to low renal perfusion, that is, due to low blood pressure or hypovolemia.[28] Another stimulant of aldosterone is increased potassium levels.[28–30] Increased aldosterone levels are associated with cardiovascular damage[31] and insulin resistance in patients with type 2 diabetes.[32]

Recently, a prospective study was performed to investigate the change and variability of copeptin in relation to serum osmolality in children with T1D treated for DKA.[33] Although osmolality increased again toward study end, probably explained by the careful switch from intravenous to subcutaneous insulin, copeptin and osmolality showed an initial parallel decline during rehydration therapy. This suggests a short degradation half-life of copeptin (as reported for the actual active hormone vasopressin[34,35]), allowing quick physiological response to correction of hyperosmolality. Using an empirical mixed-effects modeling

approach, an exponential relationship between osmolality and copeptin concentrations was characterized. High interindividual variability (IIV) in copeptin levels and its relationship with osmolality could partly be explained by different physiology in patients with known versus newly diagnosed T1D. Whether similar relationships exist between aldosterone and hypovolemia during the treatment of DKA is not known. Also, the physiological effect of the renewed increase in osmolality toward study end on copeptin secretion has not been investigated. Development of integrated pharmacometric kinetic/dynamic models, separating processes of hormone secretion and degradation, would enhance biological interpretation of model parameters. Such models could provide a physiological basis to evaluate copeptin and aldosterone as potential markers for the monitoring of treatment effects in children with T1D and DKA.

We therefore aimed to extend the aforementioned work[33] and further improve our understanding of copeptin and aldosterone regulation during rehydration treatment for DKA in children with T1D by using a physiologic semimechanistic modeling approach. Specifically, we aimed to investigate (a) the kinetic/dynamic relationship of copeptin secretion in response to the correction of hyperosmolality and (b) of aldosterone secretion in response to the correction of hypovolemia and (c) explore the association of hormone-level variability with individual patient characteristics, which potentially influence hormonal regulation.

METHODS

Clinical study design and measurements

Data originated from a prospective, observational, multicenter study performed at the University Children's Hospital of Basel (UKBB), Basel, Switzerland, and Perth Children's Hospital, Perth, Australia, between 2015 and 2019. The study was approved by local ethical committees. Children aged 1–18 years with known or newly diagnosed T1D treated for DKA were included. Patients received intravenous rehydration therapy (start of the study) and intravenous or subcutaneous insulin 1 h after start of rehydration according to hospital DKA treatment protocol derived from international guidelines.[1,36] Blood samples to measure copeptin ($n = 14$ per patient), plasma osmolality ($n = 14$), and aldosterone ($n = 6$) were taken at predefined timepoints 0–72 h after the start of rehydration. Suspected erroneous osmolality measurements (defined as >360 mOsm/kg or >10% deviation from preceding measurement, as stated previously[33]) were initially excluded from the analysis. Detailed descriptions of

measurement techniques and study design are described elsewhere.[33,37]

To include a variable on hypovolemia in this analysis, intravenous infusion rates of rehydration treatment protocol were used to calculate the expected fluid deficit over time for each patient[1]:

$$\text{Def}(t) = \text{Def}_{\text{start}} - \left(\frac{\text{infused fluid } (t)}{\text{weight}} \right) * 100\% \quad (1)$$

$$\text{If Def}(t) < 0\% \text{ then Def}(t) = 0\%$$

where $\text{Def}(t)$ is the calculated fluid deficit (%) at time t(h), $\text{Def}_{\text{start}}$ is the calculated fluid deficit (%) at study start according to DKA severity (mild DKA [pH: 7.21–7.3], 5%; moderate DKA [pH: 7.1–7.2], 6.5%; severe DKA [pH < 7.1], 8.5%), weight is the patient's weight (kg) at admission, and infused fluid is the cumulative amount of fluid (L) infused from start of rehydration until time t. This approach was evaluated by correlation (Spearman ρ correlation coefficient) of $\text{Def}(t)$ with hematocrit levels over time, which was available as an indicator of hemoconcentration for a subset of patients (treated at UKBB).

Development of semimechanistic models

Turnover model structure

Two semimechanistic models describing copeptin and aldosterone kinetics in response to rehydration treatment were developed using a nonlinear mixed-effects modeling approach. To explore physiological aspects of hormonal signaling, a turnover model structure was selected a priori. It was assumed that fluctuations in hormone levels (the dependent variables) were the result of altered secretion (i.e., the zero-order secretion rate constant [pmol/h] at time t [$k_{in}(t)$]), where copeptin $k_{in}(t)$ responds to changes in osmolality from physiologic normal or reference during treatment ($\Delta \text{Osm}[t]$; independent variable), whereas aldosterone $k_{in}(t)$ responds to changes in hydration status (fluid deficit, $\text{Def}[t]$; independent variable). The general turnover model[38–40] structures used to describe copeptin and aldosterone kinetics were defined as the following:

$$\frac{d}{dt} x(t) = k_{in}(t) - k_{out} \cdot x(t) \quad (2)$$

$$x(t = 0) = \frac{k_{in}(t = 0)}{k_{out}} \quad (3)$$

$$[x(t)] = \frac{x(t)}{V_d} \quad (4)$$

$$k_{out} = \frac{\ln(2)}{t_{1/2}} \quad (5)$$

where $\frac{d}{dt}x(t)$ is the change in the amount of copeptin or aldosterone (pmol) at time t(h), k_{in} is the zero-order secretion rate constant (pmol/h) at time t, k_{out} is the first-order degradation rate constant (h^{-1}), [$x(t)$] is the concentration (pmol/L), V_d is the distribution volume (L), and $t_{1/2}$ is the turnover half-life (h).

As copeptin and aldosterone V_d and $t_{1/2}$ are unidentifiable with the current study design, they were fixed to the literature values. Copeptin V_d was set to the extracellular fluid volume (ECF),[41] calculated as the following[42,43]:

$$ECF = 0.0215 \cdot weight^{0.647} \cdot height^{0.724} \quad (6)$$

One individual's missing height was imputed from the World Health Organization growth charts using known weight and age.[44] Because copeptin is a peptide, which generally are considered to have fast turnover $t_{1/2}$ ($\leq$10 min),[41] its $t_{1/2}$ was fixed to 0.1 h. Aldosterone V_d and $t_{1/2}$ were fixed to values reported for fludrocortisone, an aldosterone analog, of 1.11 L/kg and 1.4 h, respectively.[45]

Dynamic relationship with independent variables

Linear, exponential, and (sigmoid) maximum effect (E_{max}) relationships (both additive and proportional) were tested to describe the dynamics between changes in the independent variables, $\Delta Osm(t)$ or Def(t), and the increase in copeptin or aldosterone secretion rate, respectively, as shown with the following example:

$$k_{in}(t) = k_{in} \cdot e^{\beta * IDV(t)} \quad (7)$$

where k_{in} is the zero-order secretion rate constant (pmol/h) for normal hydration status (Def[t] = 0%) or normal reference osmolality (Osm[t] = Osm$_{ref}$), β is the dynamic slope (mOsm/kg $^{-1}$ or %$^{-1}$ in this example), and IDV(t) is the independent variable, Def(t) or $\Delta Osm(t)$, with $\Delta Osm(t)$ = Osm(t) − Osm$_{ref}$, where Osm$_{ref}$ corresponds to the individual normal reference osmolality. All tested dynamic relationships are listed in the Supporting Information.

Two different approaches for continuous incorporation of Osm(t) were tested (a) from individual osmolality predictions using a previously reported model (predicting an exponential decline to normal osmolality at study end)[33] and (b) by linear interpolation of observed values (accounting for renewed increase in osmolality at study end, as described in the Introduction). Both approaches hence allowed imputation of missing osmolality samples (see Appendix S1).

Stochastic and error model structure

Variability in the data was captured as random IIV and residual unexplained variability (RUV). IIV (log-normally distributed) was a priori included for all estimated parameters, except for those fixed to literature values, and removed when estimates approximated 0. Proportional, additive, or combined error structures were considered to describe RUV.

Model development and evaluation

Tested model structures were numerically evaluated with the Akaike information criterion (AIC) and the drop in objective function value (−2x log-likelihood) for nested models (with a change in objective function value [ΔOFV]>3.84 corresponding to $p < 0.05$ using the likelihood ratio test), relative standard error (RSE; target: <50%) of parameter estimates, and model condition number of the correlation matrix (target <1000). Visual evaluation included standard goodness-of-fit (GOF) plots, inspection of eta distributions (considering eta shrinkage), and visual predictive checks (VPCs).

To illustrate and compare the dynamic relationships of tested model structures or independent variables (simulated vs. observed osmolality), conceptual model simulations were performed for a typical individual (without the inclusion of IIV and V_d based on median population demographics).

Sensitivity analyses

Sensitivity analyses were performed to test the influence of chosen literature values of $t_{1/2}$ on estimated model parameters. Both shorter and longer $t_{1/2}$ values within a physiological plausible range were tested: for copeptin values between 1 min to 1 h (covering reported alternative $t_{1/2}$ values of 26 and 36 min[17,46]) and for aldosterone 12–126 min (covering values from 0.2 h for aldosterone up to the range of 1.6–2.6 h for fludrodrocortisone[47–49]). Copeptin model parameters were also estimated including osmolality outliers to assess if they introduced a bias.

Correlation of model parameters with patient characteristics

As developing a covariate model was not an outcome of interest, correlation of individual model parameters with potential covariates was only analyzed in a descriptive manner (numerically and visually). Investigated covariates included weight, age, DKA severity, known/unknown T1D diagnosis at admission, sex, and study center for both copeptin and aldosterone. For aldosterone, baseline

osmolality, potassium, sodium, and blood pressure (diastolic and systolic) levels were additionally evaluated. Correlations with continuous and categorical covariates were calculated with the Spearman ρ correlation coefficient and with Wilcoxon tests with a normal approximation, respectively (significance level, 5%).

Data management

Data analysis, processing, and visualization were performed in R (Version 4.0.3, R Development Core Team, Vienna, Austria).[50] Model development and simulation was done in NONMEM (Version 7.4.3, Icon Development Solutions, Ellicott City, MD)[51] using the Pirana interface (Version 2.1.0, Certara, Raleigh, NC).[52]

RESULTS

Patient characteristics and measurements

In total, 299 copeptin samples were available from 28 patients (median [minimum–maximum] 11 [7–14] per patient) (median [interquantile range, IQR] age 11.5 [8–14] years, weight 35.5 [32.0–50.5] kg, n [%] newly diagnosed T1D 20 [71.4], n [%] with mild/moderate/severe DKA 3 [10.7]/13 [46.4]/12 [42.9]),[33] of which 20 patients also had a total of 92 aldosterone measurements (median [minimum–maximum] 5 [5-6] per patient) (median [IQR] age 12 [9.8–14] years, weight 36 [33–49] kg, n [%] newly diagnosed T1D 14 [70%], n [%] with mild/moderate/severe DKA 1 [5]/9 [45]/10 [50]).[33,37] Nine copeptin samples had missing osmolality measurements (at times [number of samples] 3 [1], 6 [3], 8 [1], 10 [1], 24 [1], 48 [2] h across six patients).

The calculated fluid deficit at each aldosterone measurement timepoint is summarized in Table S1. The respective mean fluid deficit at study start was 7.2% (95% confidence interval [CI], 6.6–7.8), and the mean time to correction was 28.2 h (95% CI, 21.8–34.7). When calculated for each copeptin measurement (i.e., the whole population), the fluid deficit was 6.9% (95% CI, 6.3–7.4), and the mean time to correction was 22.5 h (95% CI, 19.6–25.4). The calculated fluid deficit correlated significantly with hematocrit levels (coefficient, 0.66; $p < 0.001$).

Developed semimechanistic models

Osmolality-dependent copeptin model

Using model-predicted osmolality[33] as an independent variable, an additive (sigmoid) E_{max} relationship

performed best in terms of AIC; however, parameter estimates could not be estimated with good confidence (unsuccessful covariance steps, $E_{max} > 3 \cdot 10^4$ pmol/h or concentration producing 50% of Emax (EC50) $\gg$ max. predicted ΔOsm). An exponential relationship was statistically preferred over an (additive) linear relationship (change in AIC [ΔAIC] = −39.2, smaller residual error and IIV). The proportional error structure was found to describe the RUV best. Model parameters are listed in Table 1 (Copeptin Model 1 [CM1]).

Using observed (interpolated) osmolality as a time-varying independent variable in the same structural model resulted in large uncertainty for all model parameters (RSE > 50%) and incorrectly predicted a rise in copeptin values toward study end. The AIC was also much higher compared with the predicted osmolality input (ΔAIC = 97.7, where nine copeptin samples with missing osmolality measurements were excluded in both model fits to allow AIC comparison). Model parameters (Copeptin Model 2 [CM2]) are listed in Table 1.

Mispredictions could be corrected assuming changing sensitivity during the study. The response to osmolality changes was set to be absent (i.e., $\beta = 0$) (A) empirically after 30 h based on visual inspection of the data and (B) after the time at which individual patients were expected to be rehydrated (fluid deficit reaches 0%). Both approaches significantly improved model predictions (ΔOFV = −111.1 and −112.8, respectively; $p < 0.001$). Considering Approach B (further referred to as Copeptin Model 3 [CM3]; VPCs as shown in Figure 1), the use of individual interpolated osmolality as a time-varying independent variable performed better compared with the use of individual predicted osmolality (ΔAIC = −6.1), and IIV and RUV were estimated to be smaller (model parameters, Table 1; GOF plots, Figure S1). Estimation of two separate β parameters before and after these timepoints resulted in the second β estimate approaching zero. Estimation of the timepoint at which β switches to 0 was also not possible (the resulting parameter value did not change from its initial estimate), nor was the estimation of two different Osm_{ref} values.

NONMEM code of CM3 is available in Appendix S1, and the model structure is visualized in Figure 2a. Differences in dynamic relationships between the three discussed model approaches are illustrated in Figure 3.

Fluid deficit–dependent aldosterone model

Similar as for copeptin, only linear and exponential relationships of Def(t) with aldosterone secretion allowed for reliable parameter estimation. A (proportional) linear relationship performed better statistically than an exponential relationship (ΔAIC = −7.0), but GOF plots indicated large

TABLE 1 Parameter estimates of key copeptin models (CMs) based on predicted and observed osmolality

| Model | Predicted osmolality | | Observed osmolality | | | |
| | CM1 | | CM2: no time-dependent slope | | CM3: β = 0 when fluid deficit = 0% | |
	Estimate [rse%]	IIV: CV%[rse%] (shrinkage%)	Estimate [rse%]	IIV: CV%[rse%] (shrinkage%)	Estimate [rse%]	IIV: CV%[rse%] (shrinkage%)
$t_{1/2}$ (h)[a]	0.1 FIX	–	0.1 FIX	–	0.1 FIX	–
k_{in} (pmol/h)	878 [13]	74.8 [11] (1)	892 [1637]	64 [104] (11)	783 [12]	60 [22] (6)
β ([mOsm/kg]$^{-1}$)	0.0669 [16]	78 [16] (10)	0.0456 [680]	89 [96] (14)	0.0461 [16]	75 [14] (12)
$\rightarrow 2 \cdot k_{in}$ (mOsm/kg)[a]	10.3	–	15.2	–	15.0	–
Osm_{ref} (mOsm/kg)	–	–	290 [70]	1 [256] (65)	285 [1]	3 [25] (24)
V_d (L)[a]	Individual ECF (median [IQR]: 8.3 [6.8–10.9])	–	Individual ECF (median [IQR]: 8.3 [6.8–10.9])	–	Individual ECF (median [IQR]: 8.3 [6.8–10.9])	–
Residual error (CV%)	41 [9] (7)	–	48 [42] (6)	–	38 [8] (9)	–

Abbreviations: $2 \cdot k_{in}$, calculated increase in osmolality responsible for a twofold increase in the zero-order secretion rate constant; β, dynamic slope; CV, coefficient of variation calculated as CV $= \sqrt{e^{\omega^2} - 1} \cdot 100\%$, where ω^2 is the estimated variance of a log-normal distribution for IIV, and for the residual error the CV represents the square root of the residual variance; ECF, extracellular fluid; IIV, interindividual variability; IQR, interquantile range; k_{in}, zero-order secretion rate constant; Osm_{ref}, reference osmolality; rse, relative standard error; $t_{1/2}$, turnover half-life; V_d, volume of distribution.

[a]Parameters were not estimated in the model but either derived from an estimated parameter ($2 \cdot k_{in}$), taken from the literature ($t_{1/2}$), or based on population demographics (V_d).

bias over time (overprediction at treatment start, increasing underprediction and again overprediction at study end).

This bias could be corrected by an extended model structure assuming an upstream intermediate signal with slower turnover compared with the relatively short aldosterone $t_{1/2}$ (Figure 1b). Def(t) was assumed to alter the production rate of this intermediate signal, and the aldosterone k_{in} was assumed to be directly proportional to the relative amount of this signal (see Appendix S1). With this model structure, the exponential relationship resulted in a better model fit compared with additive and proportional linear relationships (ΔAIC = −11.0 and ΔAIC = −8.3, respectively), RUV was largely reduced (36% vs. 51% in the reference model without extension; ΔAIC = −52.8), and unbiased kinetic and dynamic predictions were obtained. To further increase model stability, IIV on the k_{in} was removed, as inclusion was associated with large RSE in other model parameters (Aldosterone Model 1 [AM1]). In a second step, k_{in} was fixed (priorly estimated to be 6150 pmol/h) to the value required to reach the normal reference range (5049 pmol/h; i.e., the median value of the reference range of 1083 to 8120 pmol/h for the lower and upper limits, respectively; Table 2 [Aldosterone Model 2, AM2]), as its estimation was associated with a high condition number and high correlation between parameter estimates (as normal aldosterone range was not reached at the end of the study, k_{in} is probably unidentifiable). In this range of k_{in}, the signal $t_{1/2}$ and β were estimated between 18.7 (RSE%: 16) and 13.4 (17) h and 0.647 (4)–0.36 (6) %$^{-1}$, respectively. A proportional error structure was preferred over additive and combined error structures throughout the modeling.

Model evaluation of AM2 through VPCs are shown in Figure 1, GOF plots are shown in Figure S2, and parameter estimates for the models with estimated (AM1) and fixed k_{in} (AM2) are listed in Table 2. The AM1 model structure is visualized in Figure 2b, and the code is available in Appendix S1. The dynamic relations between fluid deficit, intermediate signal production and aldosterone secretion, and the improvement in model predictions as a result of the extension are illustrated in Figure 4.

Sensitivity analyses

Model parameter estimates resulting from copeptin and aldosterone $t_{1/2}$ sensitivity analyses are listed in Tables S2 and S3, respectively. The estimated copeptin secretion rate reduced expectedly (from 878 to 84.2 pmol/L) with increasing $t_{1/2}$ (from 0.1 to 1 h), whereas β, IIV, and RUV did not change significantly. Inclusion of osmolality outlier data did not result in significantly different parameter

estimates. Similarly, for aldosterone, estimated signal $t_{1/2}$ decreased nonsignificantly (from 16.3 to 15.3 h) with increasing aldosterone $t_{1/2}$ (from 12 to 126 min), and other parameters, such as β, IIV, and RUV, remained unchanged.

Association of hormone-level variability with covariates

Correlations between patient demographics and individual model parameter estimates are shown in Figure 5,

and numerical details are given in Tables S4 and S5. In the copeptin model, diagnosis was significantly correlated with β and k_{in} (steeper response and lower secretion in patients with known T1D), and DKA partly showed associations with Osm_{ref}. Weight and age were initially significantly correlated with k_{in}, but further inspection showed that this represented a bias introduced by the weight-based scaling of V_d (ECF calculated based on weight and height). When V_d was set to the ECF (8.2 L) of the average individual (35.5 kg, 152 cm), only correlations with diagnosis and DKA remained significant; weight-based scaling of both secretion and V_d parameters gave similar
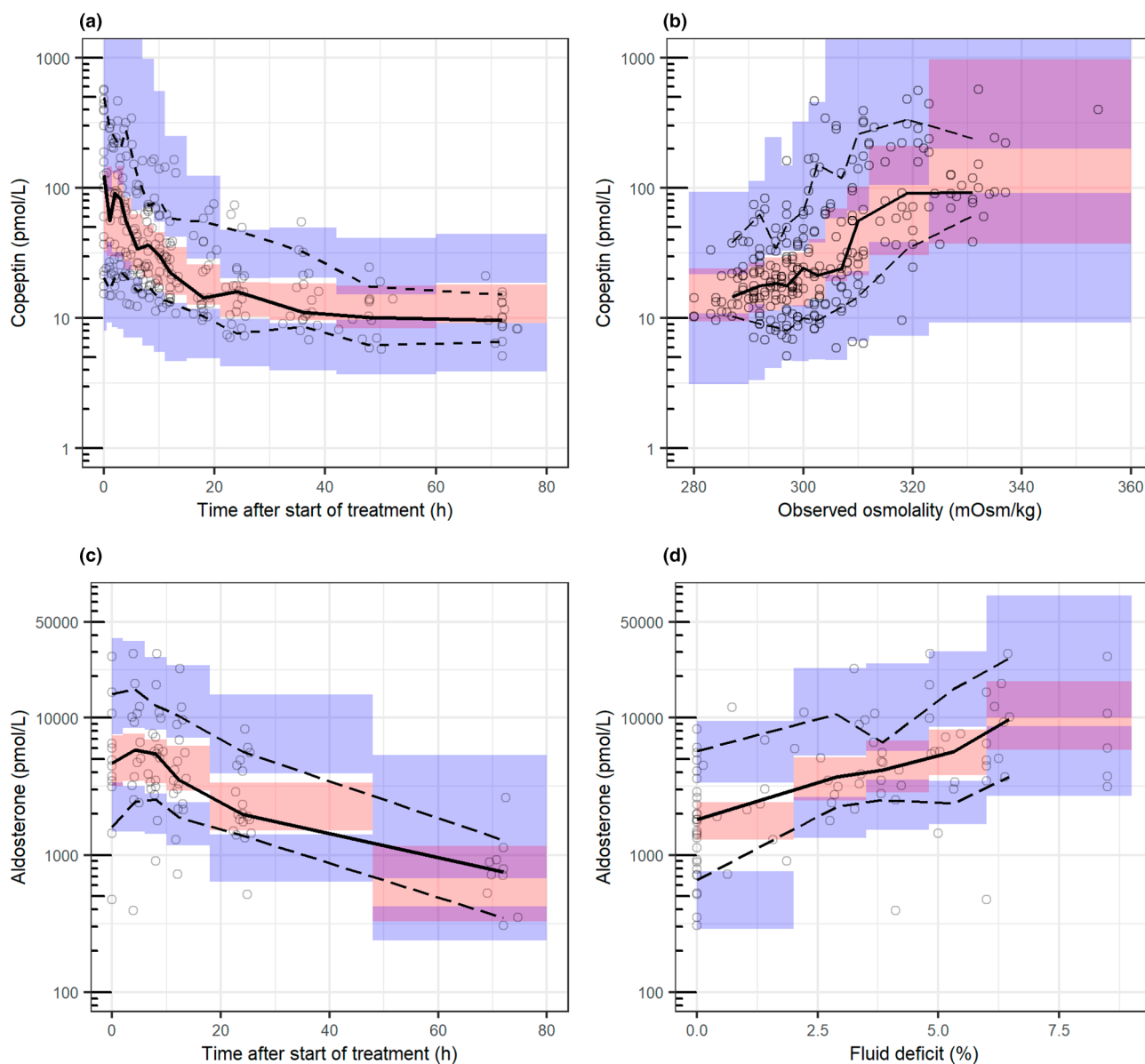
FIGURE 1 Visual predictive checks of copeptin and aldosterone models (Copeptin Model 3 and Aldosterone Model 2, respectively): (a) copeptin concentration versus time, (b) copeptin concentration versus osmolality, (c) aldosterone concentration versus time, and (d) aldosterone concentration versus calculated fluid deficit. The observed concentrations are depicted as black open dots, and the empirical median and 80% prediction interval of the data are shown with the thick and thin black lines. The shaded areas represent the 95% confidence interval of the median and 80% prediction interval of the simulated data for each bin, originating from 1000 model runs.
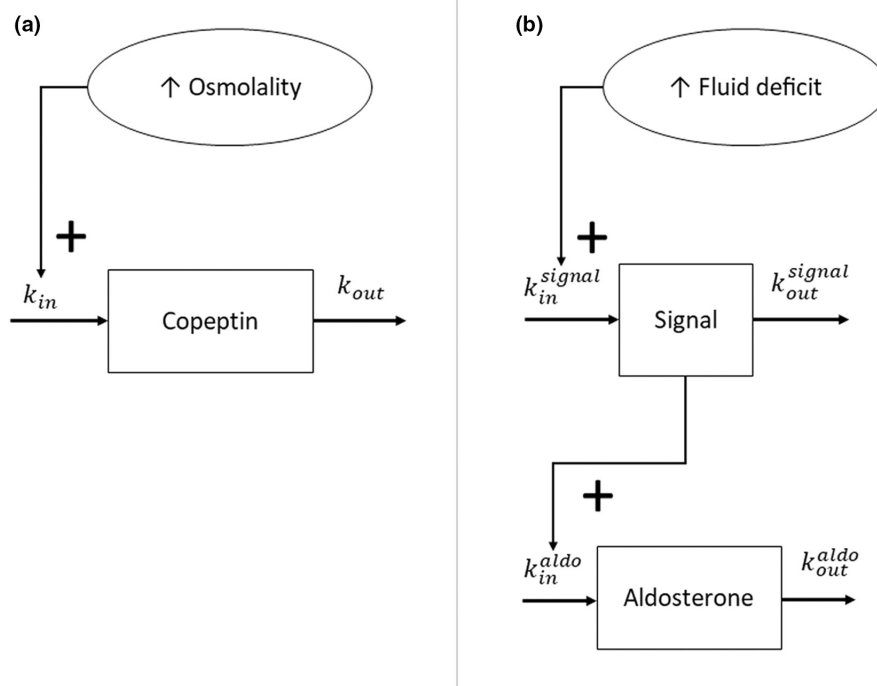
FIGURE 2 Schematic representation of structural turnover models to describe copeptin and aldosterone kinetics. General turnover model structures which link the independent variable (shown in the circle) to the hormone secretion rate (k_{in}) through a stimulatory exponential dynamic relationship. The box represents the amount of hormone at a certain time, which is determined by its secretion and degradation rate, represented as zero- and first-order rates, respectively (k_{in} [pmol/h] and k_{out} [h^{-1}]). (a) Copeptin models (CM2/3) based on simulated or observed interpolated osmolality as an independent variable, where CM3 has a rehydration dependent dynamic slope. (b) Aldosterone models (AM1/2) with an extended turnover model structure. The independent variable, the fluid deficit, stimulates the production rate of an intermediate signal (i.e., zero-order rate constant, k_{in}^{signal} [signal]/h) through an exponential dynamic relationship. The aldosterone secretion rate (k_{in}^{aldo}) is directly proportional to the relative abundance of this signal.

results. In the aldosterone model, weight was significantly correlated with the slope β (larger response to changes in fluid deficit with lower weight). Removal of weight-based scaling of V_d (use of average weight/V_d) still gave similar results. No significant correlation with potassium levels or blood pressure was found.

DISCUSSION

This study is the first to compare the kinetic/dynamic profiles of copeptin (as surrogate marker for AVP) in response to the correction of serum osmolality and aldosterone in response to the correction of hypovolemia (quantified as fluid deficit) during rehydration treatment for DKA in children with T1D through a semimechanistic modeling approach. This revealed large differences between the two hormones: Due to the relatively fast turnover $t_{1/2}$ of both hormones, copeptin dynamics were described with a fast relationship (immediate effect of osmolality on copeptin secretion rate, with decreased sensitivity after full rehydration), yet the aldosterone dynamic response was delayed and could only be

well characterized by the addition of a slow turnover compartment representing an upstream signal on aldosterone secretion. Furthermore, variability in copeptin dynamics could partly be attributed to differences between patients with known versus new T1D diagnosis, whereas aldosterone dynamics as a response to fluid deficit was weight dependent. This suggests that copeptin (fast response), but not aldosterone (delayed response), may be further evaluated as a marker for DKA rehydration protocol optimization, for example, to decrease the risk of cerebral edema. Suggested chronic upregulation of aldosterone deserves further investigation, as associated with cardiovascular risk and insulin resistance in other populations.[31,32]

Best copeptin predictions were obtained using interpolated osmolality as an independent variable for copeptin secretion and assuming reduced sensitivity to iatrogenic osmolality increase after approximately 23 h, although minor overprediction at the end of the study remained (Figure 1a). The change in dynamics is probably due to an osmotic shift introduced by hypovolemia, which possibly increases sensitivity of the osmoreceptor during DKA: The osmotic threshold for a response would be accordingly
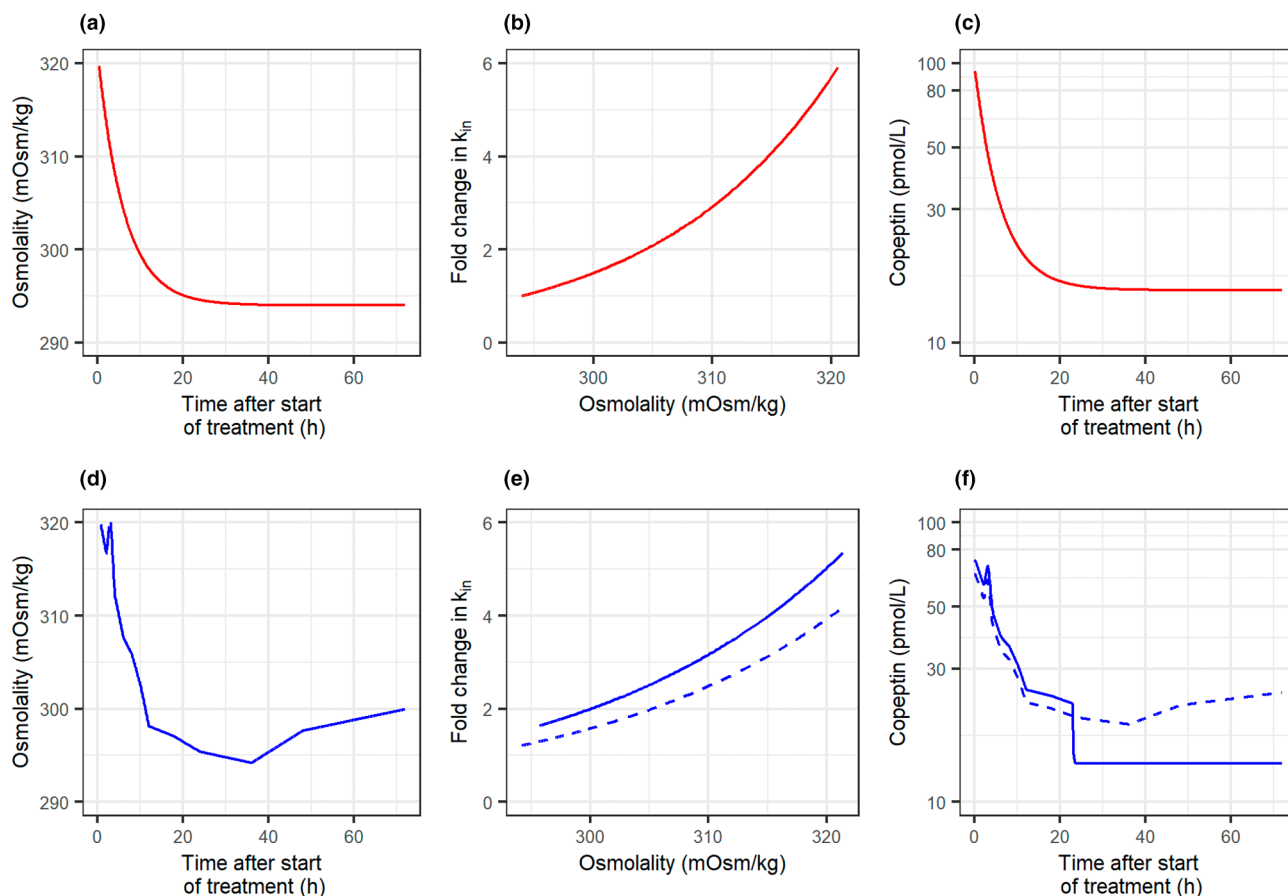
FIGURE 3 Conceptual copeptin model (CM) simulations for a typical individual. (a–c) CM1 (i.e., simulated osmolality as independent variable), (d–f) CM2 (solid line; i.e., observed osmolality as independent variable), and CM3 (dotted line; i.e., observed osmolality as an independent variable with rehydration-dependent dynamics). (a/d) Change in osmolality over time, (b/e) relative increase in copeptin secretion rate over change in osmolality, (c/f) predicted copeptin concentrations over time. k_{in}, zero-order secretion rate constant.

TABLE 2 Parameter estimates of extended key aldosterone models (AMs) with estimated and fixed reference secretion rate (k_{in})

Reference secretion rate	Estimated aldosterone k_{in} (AM1)		Fixed aldosterone k_{in} (AM2)	
	Estimate [rse%]	IIV: CV% [rse%] (shrinkage%)	Estimate [rse%]	IIV: CV% [rse%] (shrinkage%)
Aldosterone $t_{1/2}$ (h)[a]	1.4 FIX	–	1.4 FIX	–
Signal $t_{1/2}$ (h)	14.8 [2]	54 [77] (19)	15.7 [13]	53 [22] (19)
Aldosterone k_{in} (pmol/h)	6150 [9]	–	5049.1 FIX[b]	–
β (%$^{-1}$)	0.417 [4]	16 [11] (8)	0.441 [5]	18 [16] (5)
→2·signal k_{in} (%)[a]	1.66	–	1.57	–
V_d (L/kg)[a]	1.11 FIX	–	1.11 FIX	–
Residual error (CV%)	36 [15] (14)	–	36 [11] (15)	–

Abbreviations: 2· signal k_{in}, calculated increase in fluid deficit responsible for a twofold increase in the zero-order signal production rate constant; β, dynamic slope; CV, coefficient of variation calculated as $CV = \sqrt{e^{\omega^2} - 1} \cdot 100\%$, where ω^2 is the estimated variance of a log-normal distribution for IIV, and for the residual error the CV represents the square root of the residual variance; IIV, interindividual variability; k_{in}, zero-order secretion rate constant; rse, relative standard error; $t_{1/2}$, turnover half-life; V_d, volume of distribution.

[a]Parameters were not estimated in the model but either derived from an estimated parameter (2·k_{in}) or taken from the literature ($t_{1/2}$, V_d).

[b]k_{in} was fixed to a value corresponding to the median concentration of the laboratory reference range (x): $k_{in} = x \cdot V_d \cdot k_{out}$, where V_d is based on the average patient (1.11 L/kg · 35.5 kg), and k_{out} is the degradation rate based on the fixed $t_{1/2}$ (ln[2]/1.4 h).
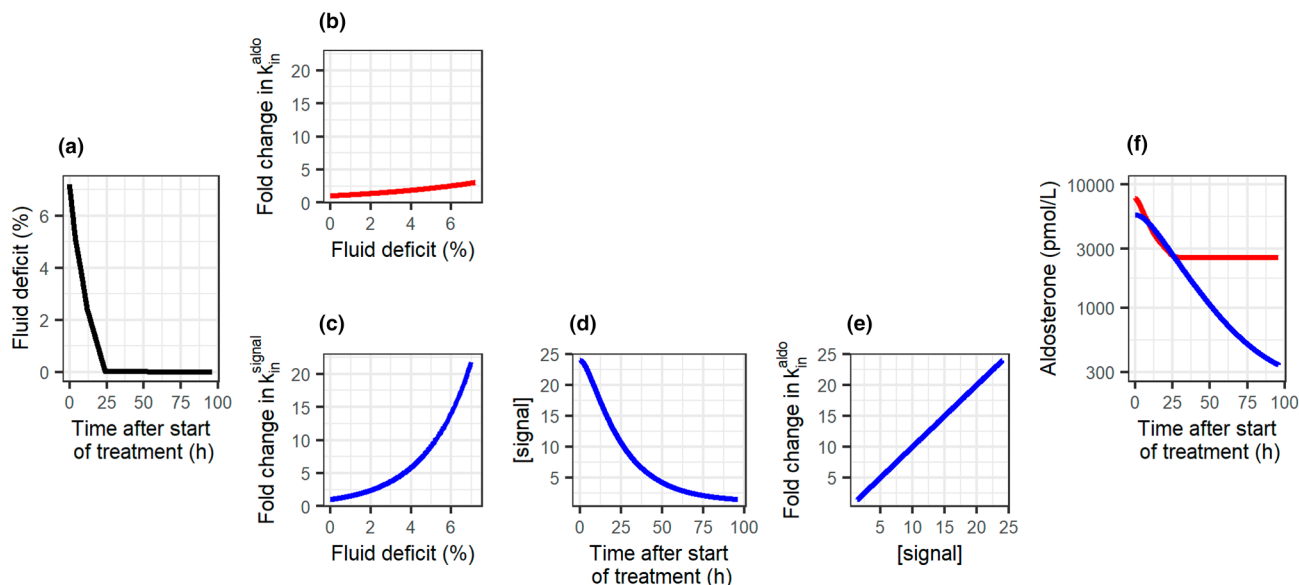
FIGURE 4 Conceptual aldosterone model simulations for a typical individual. (a, b, f) Initial model structure (indicated in red). (a, c–f) Aldosterone Model 2 (i.e., extended model structure, indicated in blue). (a) Calculated fluid deficit over time, (b) relative increase in aldosterone secretion rate over fluid deficit, (c) relative increase in signal production rate over fluid deficit, (d) relative amount of signal over time, (e) relative increase in aldosterone secretion rate over relative signal amount, and (f) predicted aldosterone secretion over time. k_{in}^{signal}, zero-order signal production rate constant; k_{in}^{aldo}, zero-order aldosterone secretion rate constant.

expected to be lower in a hypovolemic state compared with normovolemia.[13] Estimation of different thresholds (e.g., Osm_{ref}) was not possible, as well as estimation of a different β after expected fluid deficit correction other than 0. Resolution of insulin deficiency during DKA treatment could also explain a sensitivity change, as insulin deficiency has been demonstrated to stimulate AVP secretion in patients with diabetes mellitus.[53] However, insulin administration started 1–2 h after initiation of rehydration, and glucose levels normalized before 20 h,[33] whereas the sensitivity change was observed between 23 h (average expected full rehydration of study population) to approximately 30 h (visual assessment). Lastly, the reduction of stress-related factors over time such as nausea and emesis, known to influence copeptin secretion, could also explain the difference in dynamics.[18–20] Therefore, the use of copeptin as a marker for rehydration individualization to reduce the risk of acute events such as cerebral edema does have potential but requires more research to fully elucidate the impact of such a possible osmotic shift.

The investigation of possible covariates showed that weight-based scaling of the copeptin V_d was unnecessary or that both secretion and volume should be allometrically scaled, respectively. The significant association of T1D diagnosis with the copeptin dynamics seen previously[33] is suspected to be linked to potential osmoreceptor and AVP-receptor insensitivity in newly diagnosed T1D patients, who develop DKA over longer time periods and are exposed to the hyperosmolar hypovolemic state longer

than known T1D patients. The association of DKA severities with Osm_{ref} is harder to interpret because of the low number of patients with mild DKA ($n = 3$) and the lack of significant associations wbetween DKA (moderate vs. severe) and Osm_{ref}.

The decrease in aldosterone levels was delayed, and good predictions could be obtained only after introducing an extra turnover compartment, likely representing an upstream intermediate signal responsible for chronic aldosterone upregulation (as opposed to well-known acute regulation by the RAAS system). As chronically high aldosterone levels are associated with cardiovascular risks, it is important that the exact cause be elucidated with future research.[31] It has been found that chronic exposure to high angiotensin II and potassium increases the expression of cytochrome P450 1B2 (CYP11B2) coding for aldosterone synthase.[54] Because CYP enzymes generally have a longer $t_{1/2}$ (range, 2–806 h[55]) than peptides (<10 min[41]), the additional compartment might correspond to an increased expression of CYP11B2. Our study may provide a first, rough estimate for its turnover $t_{1/2}$, in the range of 13.4 h (95% CI, 8.9–17.9) to 18.7 h (95% CI, 12.8–24.6), considering sensitivity analyses. Currently, aldosterone synthase is being investigated as a pharmacological target for the treatment of hypertension and hyperaldosteronism, and some phase II studies have already been executed.[56] Therefore, these results could be of use for the description and/or prediction of the pharmacokinetics and pharmacodynamics of such (future) aldosterone synthase inhibitors. Due to this
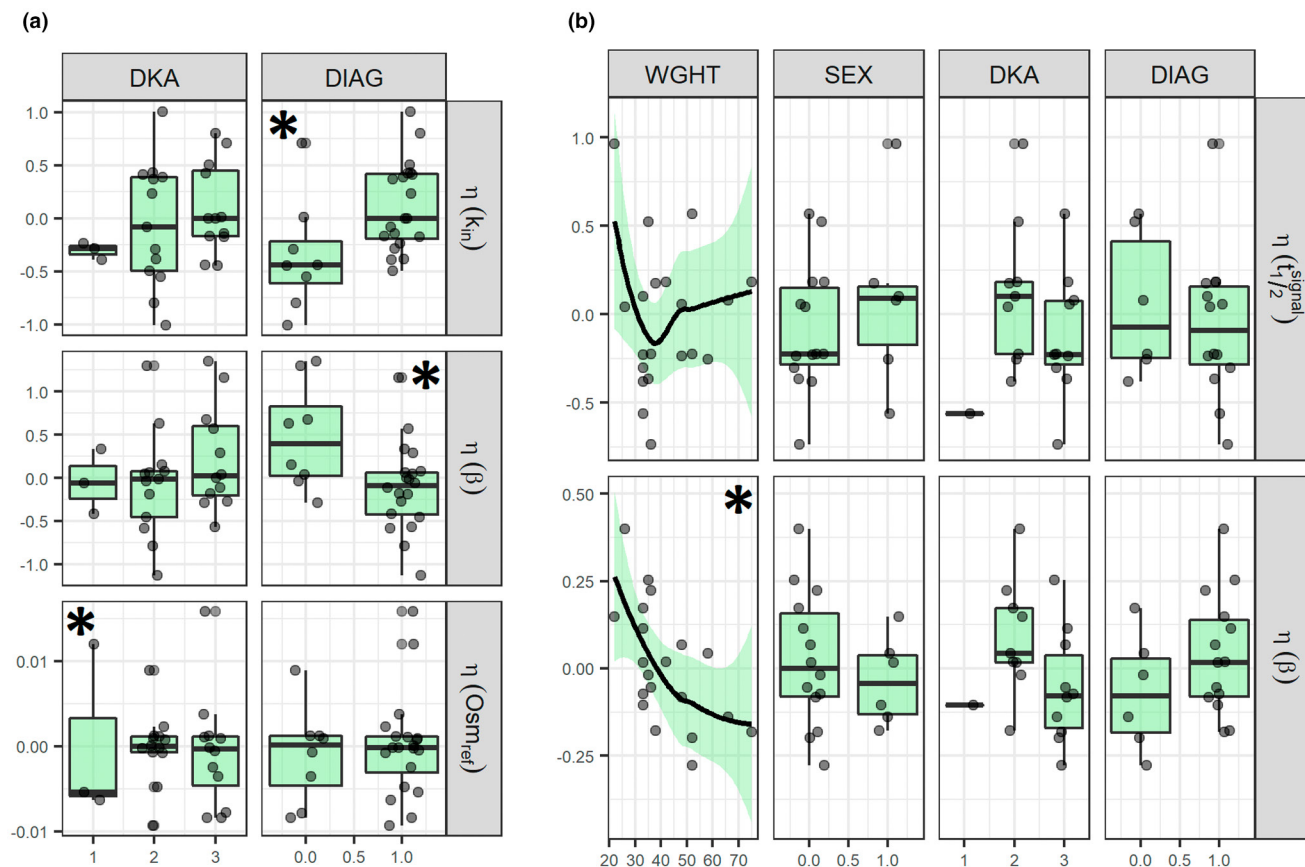
FIGURE 5 Visualized associations between individual model parameters and possible covariates for (a) Copeptin Model 3 and (b) Aldosterone Model 2. Copeptin distribution volume was set to the average extracellular fluid of the population (8.2 L). Significant covariate relationships are indicated with an asterisk (see Tables S4 and S5). Continuous variables are shown with a nonparametric regression line (loess) and 95% confidence interval, and categorical variables are shown with boxplots. η, individual random effect; β, dynamic slope parameter ($mOsm^{-1}$ or $\%^{-1}$ for the copeptin or aldosterone model, respectively); DIAG, type 1 diabetes diagnosis (0 = known, 1 = new); DKA, diabetic ketoacidosis severity (1 = mild, 2 = moderate, 3 = severe); k_{in}, zero-order copeptin secretion rate constant (pmol/h); SEX, gender (0 = male, 1 = female); $t_{1/2}^{signal}$, signal turnover half-life (h); WGHT, weight (kg).

delay, the application of monitoring changes in aldosterone levels during DKA rehydration as a marker for treatment individualization is much less promising.

It was found that only weight was significantly correlated with the variability in aldosterone β, independent of the allometric scaling approach of V_d and/or secretion. This indicates that patients with lower weight respond more strongly to the same relative fluid deficit, probably in line with higher weight-based fluid requirements in smaller patients.[1] Higher aldosterone baseline concentrations in younger children, previously reported in healthy populations,[57,58] might have contributed to this observation. However, no correlation with age could be observed in our study, possibly limited by the fact that the normal reference values at the end of the study were not yet reached. Interestingly, DKA severity and known versus new T1D diagnosis did not show correlations with aldosterone secretion or sensitivity, as opposed to copeptin. Furthermore, no significant association between model parameters and potassium or blood pressure was

determined, although these factors have been described to induce aldosterone secretion,[28–30] which might be explained by the small population size.

The semimechanistic pharmacometric approach used in this study has some limitations. The turnover model structure was selected a priori to mimic hormone secretion and degradation and incorporate available knowledge. This model structure is traditionally seen as an indirect effect model to account for possible delays in effect.[38,40,59] Although a direct relationship between copeptin and osmolality in T1D patients with DKA was previously described,[33] a decrease in aldosterone levels did show a clear delay. Nevertheless, in both cases the turnover model structure allowed for a more biological interpretation of the model parameters. For instance, the predicted relative increase in secretion rate may be used to compare relative secretion in other conditions (discussed later).

Furthermore, V_d could not be estimated as no known intravenous dose was administered, and degradation $t_{1/2}$

were unidentifiable as decline rates of assumed independent variables (ΔOsm[t], Def[t]) were slower than expected degradation rates according to the literature. Hence, absolute values of secretion rates reported should only be interpreted regarding assumptions made for those two parameters. Nevertheless, the use of V_d to scale the hormone amounts instead of modeling the concentration data allows for the comparison of estimated secretion rates of copeptin (secreted in equimolar amount as vasopressin) during DKA to pharmacological dosing rates of vasopressin, for instance, in the context of catecholamine-refractory shock.[60] A usual dose of 0.01–0.03 IU/h Empressin®(OrPha Swiss GmbH) would be equal to 1840–5521 pmol/h (where 40 IU is 133 µg with a molecular weight of 1084 g/mol),[60] which would be higher than the estimated normal secretion rate of 783–878 pmol/h in the normo-osmolar state, yet much less when compared with the expected sixfold increase in secretion rate during DKA (Figure 3).

Hypovolemia was quantified through calculated fluid deficit according to DKA severity, as precise data on dehydration (e.g., by repeated weight assessments or fluid balance) is difficult to collect in clinical routine. It is still an ongoing debate whether DKA severity properly predicts fluid deficit.[61] Real-time data on infused fluids and amounts, renal clearance, and hemoconcentration may be used for volume kinetic modeling in future studies to get an even more accurate estimate of water balance in patients over time.[62,63]

To conclude, this semimechanistic pharmacometric analysis provided novel physiologic insights into hormonal regulation during rehydration treatment for DKA. The results suggest that copeptin, but not aldosterone, may be further evaluated as an acute marker for DKA rehydration protocol optimization, for example, to further reduce the risk of complications such as cerebral edema. Suggested chronic upregulation of aldosterone deserves further investigation in the population of patients with T1D with respect to cardiovascular risks and insulin resistance. Although more research is required to address generated hypotheses, model-derived parameters (e.g., relative increase in hormone secretion, dynamic slope) and determined covariates can already be of interest for future research on different conditions and allow the quantitative comparison of water hormone regulation.

AUTHOR CONTRIBUTIONS

M.E.O. and V.G. wrote the manuscript. M.-A.B., G.S., M.P., and V.G. designed the research. M.A.B. and G.S. performed the research. M.E.O. analyzed the data.

ACKNOWLEDGMENTS

FUNDING INFORMATION

CONFLICT OF INTEREST

M. Pfister is a part-time consultant for Certara. M.E. Otto is now an employee at the Centre for Human Drug Research in Leiden, the Netherlands, where she is also pursuing her PhD in collaboration with the Leiden University Medical Centre, Leiden, the Netherlands. All other authors declared no competing interests for this work.

DUAL PUBLICATION

The clinical copeptin data has been published previously, but has not been analyzed using a semimechanistic modeling approach (Burckhardt et al. [2020] J Clin Endocrinol Metab). The clinical aldosterone data are submitted for publication together with pro-ANP data not reported here (abstract presented at European Society for Pediatric Endocrinology 2021, Burckhardt et al. [2021] Horm Res Paediatr). This article also does not present any modeling approach/results. None of the presented figures here are shown in this article, which focuses on clinical data description.

ORCID

Marije E. Otto https://orcid.org/0000-0002-5767-604X
Marie-Anne Burckhardt https://orcid.org/0000-0002-6274-5900
Gabor Szinnai https://orcid.org/0000-0003-0559-2597
Marc Pfister https://orcid.org/0000-0003-2597-1228
Verena Gotta https://orcid.org/0000-0001-6254-5207

REFERENCES

1. Wolfsdorf JI, Glaser N, Agus M, et al. ISPAD clinical practice consensus guidelines 2018: diabetic ketoacidosis and the hyperglycemic hyperosmolar state. *Pediatr Diabetes*. 2018;19:155-177.

2. Foster DW, McGarry JD. The metabolic derangements and treatment of diabetic ketoacidosis. *N Engl J Med*. 1983;309:159-169.

3. Kitabchi AE, Umpierrez GE, Murphy MB, Kreisberg RA. Hyperglycemic crises in adult patients with diabetes: a consensus statement from the American Diabetes Association. *Diabetes Care*. 2006;29:2739-2748.

4. Morgan E, Black CR, Abid N, Cardwell CR, McCance DR, Patterson CC. Mortality in type 1 diabetes diagnosed in childhood in Northern Ireland during 1989-2012: a population-based cohort study. *Pediatr Diabetes*. 2018;19:166-170.

5. Gibb FW, Teoh WL, Graham J, Lockman KA. Risk of death following admission to a UK hospital with diabetic ketoacidosis. *Diabetologia*. 2016;59:2082-2087.

6. Curtis JR, To T, Muirhead S, Cummings E, Daneman D. Recent trends in hospitalization for diabetic ketoacidosis in Ontario children. *Diabetes Care*. 2002;25:1591-1596.

7. Edge JA, Hawkins MM, Winter DL, Dunger DB. The risk and outcome of cerebral oedema developing during diabetic ketoacidosis. *Arch Dis Child*. 2001;85:16-22.

8. Edge JA. Cerebral oedema during treatment of diabetic ketoacidosis: are we any nearer finding a cause? *Diabetes Metab Res Rev*. 2000;16:316-324.

9. Glaser N, Barnett P, McCaslin I, et al. Risk factors for cerebral edema in children with diabetic ketoacidosis. *N Engl J Med*. 2001;344:264-269.

10. Tulassay T, Rascher W, Körner A, Miltényl M. Atrial natriuretic peptide and other vasoactive hormones during treatment of severe diabetic ketoacidosis in children. *J Pediatr*. 1987;111:329-334.

11. Durr JA, Hoffman WH, Hensen J, Sklar AH, el Gammal T, Steinhart CM. Osmoregulation of vasopressin in diabetic ketoacidosis. *Am J Physiol Endocrinol Metab*. 1990;259:E723-E728.

12. Schrier RW, Berl T, Anderson RJ. Osmotic and nonosmotic control of vasopressin release. *Am J Physiol – Ren Fluid Electrolyte Physiol*. 1979;236:F321-F332.

13. Robertson GL, Athar S. The interaction of blood osmolality and blood volume in regulating plasma vasopressin in man. *J Clin Endocrinol Metab*. 1976;42:613-620.

14. Robertson GL. Vasopressin in osmotic regulation in man. *Annu Rev Med*. 1974;25:315-322.

15. Morgenthaler NG, Struck J, Alonso C, Bergmann A. Assay for the measurement of copeptin, a stable peptide derived from the precursor of vasopressin. *Clin Chem*. 2006;52:112-119.

16. Szinnai G, Morgenthaler NG, Berneis K, et al. Changes in plasma copeptin, the C-terminal portion of arginine vasopressin during water deprivation and excess in healthy subjects. *J Clin Endocrinol Metab*. 2007;92:3973-3978.

17. Fenske WK, Schnyder I, Koch G, et al. Release and decay kinetics of copeptin vs AVP in response to osmotic alterations in healthy volunteers. *J Clin Endocrinol Metab*. 2018;103:505-513.

18. De Marchis GM, Katan M, Weck A, et al. Copeptin adds prognostic information after ischemic stroke: results from the CoRisk study. *Neurology*. 2013;80:1278-1286.

19. Reichlin T, Hochholzer W, Stelzig C, et al. Incremental value of Copeptin for rapid rule out of acute myocardial infarction. *J Am Coll Cardiol*. 2009;54:60-68.

20. Nickel CH, Bingisser R, Morgenthaler NG. The role of copeptin as a diagnostic and prognostic biomarker for risk stratification in the emergency department. *BMC Med*. 2012;10:7.

21. Balanescu S, Kopp P, Gaskill MB, Morgenthaler NG, Schindler C, Rutishauser J. Correlation of plasma copeptin and vasopressin concentrations in hypo-, iso-, and hyperosmolar states. *J Clin Endocrinol Metab*. 2011;96:1046-1052.

22. Christ-Crain M, Refardt J, Winzeler B. Approach to the patient: "utility of the Copeptin assay". *J Clin Endocrinol Metab*. 2022;107:1727-1738.

23. Blek N, Szwed P, Putowska P, et al. The diagnostic and prognostic value of copeptin in patients with acute ischemic stroke and transient ischemic attack: a systematic review and meta-analysis. *Cardiol J*. 2022;29:610-618.

24. Lytvyn Y, Bjornstad P, Katz A, et al. SGLT2 inhibition increases serum Copeptin in young adults with type 1 diabetes. *Diabetes Metab*. 2020;46:203-209.

25. Mu D, Cheng J, Qiu L, Cheng X. Copeptin as a diagnostic and prognostic biomarker in cardiovascular diseases. *Front Cardiovasc Med*. 2022;9:1-25.

26. Melena I, Bjornstad P, Schäfer M, et al. Serum copeptin and NT-proBNP is associated with central aortic stiffness and flow hemodynamics in adolescents with type 1 diabetes: a pilot study. *J Diabetes Complicat*. 2021;35:107883.

27. Raizada V, Skipper B, Luo W, Griffith J. Intracardiac and intrarenal renin-angiotensin systems: mechanisms of cardiovascular and renal effects. *J Investig Med*. 2007;55:341-359.

28. Horton R. Aldosterone: review of its physiology and diagnostic aspects of primary aldosteronism. *Metabolism*. 1973;22:1525-1545.

29. Simpson SA, Tait JF, Bush IE. Secretion of a salt-retaining hormone by the mammalian adrenal cortex. *Lancet*. 1952;260:226-228.

30. Pearce D, Soundararajan R, Trimpert C, Kashlan OB, Deen PMT, Kohan DE. Collecting duct principal cell transport processes and their regulation. *Clin J Am Soc Nephrol*. 2015;10:135-146.

31. Buffolo F, Tetti M, Mulatero P, Monticone S. Aldosterone as a mediator of cardiovascular damage. *Hypertension*. 2022;79:1899-1911. doi:10.1161/HYPERTENSIONAHA.122.17964

32. Bruder-Nascimento T, Da Silva MAB, Tostes RC. The involvement of aldosterone on vascular insulin resistance: implications in obesity and type 2 diabetes. *Diabetol Metab Syndr*. 2014;6:1-8.

33. Burckhardt MA, Gotta V, Beglinger S, et al. Copeptin kinetics and its relationship to osmolality during rehydration for diabetic ketoacidosis in children. *J Clin Endocrinol Metab*. 2020;105:e4169-e4178.

34. Baumann G, Dingman JF. Distribution, blood transport, and degradation of antidiuretic hormone in man. *J Clin Invest*. 1976;57:1109-1116.

35. SwissMedic. Empressin (Orpha Swiss GmbH, Küsnacht, Austria). *Product Information* (2019). https://www.swissmedicinfo.ch/?Lang=EN

36. Dunger DB, Sperling MA, Acerini CL, et al. European Society for Paediatric Endocrinology/Lawson Wilkins pediatric Endocrine Society consensus statement on diabetic ketoacidosis in children and adolescents. *Pediatrics*. 2004;113:e133-e140.

37. Burckhardt M-A, Otto M, Gotta V, et al. Aldosterone and pro-atrial natriuretic peptide kinetics in response to rehydration in children with diabetic ketoacidosis. *Horm Res Paediatr*. 2021;94:37-38.

38. Upton RN, Mould DR. Basic concepts in population modeling, simulation, and model-based drug development: part

III-introduction to pharmacodynamic modeling methods. *CPT Pharmacometrics Syst Pharmacol*. 2014;3:1-16.

39. Holford N. Pharmacodynamic principles and the time course of delayed and cumulative drug effects. *Transl Clin Pharmacol*. 2018;26:56-59.

40. Dayneka NL, Garg V, Jusko WJ. Comparison of four basic models of indirect Pharmacodynamic responses. *J Pharmacokinet Biopharm*. 1993;21:457-478.

41. Diao L, Meibohm B. Pharmacokinetics and pharmacokinetic-pharmacodynamic correlations of therapeutic peptides. *Clin Pharmacokinet*. 2013;52:855-868.

42. Peters AM. Estimation of extracellular fluid volume in children. *Pediatr Nephrol*. 2012;27:1149-1155.

43. Bird NJ, Henderson BL, Lui D, Ballinger JR, Peters AM. Indexing glomerular filtration rate to suit children. *J Nucl Med*. 2003;44:1037-1043.

44. de Onis M, Onyango A, Borghi E, Siyam A, Pinol A. *WHO child growth standards*. Department of Nutrition for Health and Development, World Health Organization; 2009. doi:10.1111/j.1469-8749.2009.03503.x

45. Hamitouche N, Comets E, Ribot M, Alvarez JC, Bellissant E, Laviolle B. Population pharmacokinetic-Pharmacodynamic model of Oral fludrocortisone and intravenous hydrocortisone in healthy volunteers. *AAPS J*. 2017;19:727-735.

46. Koch G, Schnyder I, Strauss K, et al. Model for characterizing copeptin kinetics and response in healthy subjects. 5:5.

47. Banda J, Lakshmanan R, Vvs SP, Gudla SP, Prudhivi R. A highly sensitive method for the quantification of fludrocortisone in human plasma using ultra-high-performance liquid chromatography tandem mass spectrometry and its pharmacokinetic application. *Biomed Chromatogr*. 2015;29:1213-1219.

48. Cheville RA, Luetscher JA, Hancock EW, Dowdy AJ, Nokes GW. Distribution, conjugation, and excretion of labeled aldosterone in congestive heart failure and in controls with normal circulation: development and testing of a model with an analog computer. *J Clin Invest*. 1966;45:1302-1316.

49. Mitsky VP, Workman RJ, Nicholson WE, Vernikos J, Robertson RM, Robertson D. A sensitive radioimmunoassay for fludrocortisone in human plasma. *Steroids*. 1994;59:555-558.

50. R Core Team (2020). *R: A Language and Environment for Statistical Computing*. R Foundation for Statistical Computing, . https://www.r-project.org/

51. Beal SL, Sheiner LB, Boeckmann AJ, Bauer RJ. *NONMEM Users Guides (1989–2018)*. ICON Dev. Solut. 2018.

52. Keizer RJ, Karlsson MO, Hooker A. Modeling and simulation workbench for NONMEM: tutorial on Pirana, PsN, and Xpose. *CPT Pharmacometrics Syst Pharmacol*. 2013;2:1-9.

53. Vokes TP, Aycinena PR, Robertson GL. Effect of insulin on effect of insulin on osmoregulation of vasopressin. *Am J Phys*. 1987;252:E538-E548.

54. Hattangady N, Olala L, Bollag WB, Rainey WE. Acute and chronic regulation of aldosterone production. *Mol Cell Endocrinol*. 2012;350:151-162.

55. Yang J, Liao M, Shou M, et al. Cytochrome P450 turnover: regulation of synthesis and degradation, methods for determining rates, and implications for the prediction of drug interactions. *Curr Drug Metab*. 2008;9:384-393.

56. Lenzini L, Zanotti G, Bonchio M, Rossi GP. Aldosterone synthase inhibitors for cardiovascular diseases: a comprehensive review of preclinical, clinical and in silico data. *Pharmacol Res*. 2021;163:105332.

57. Dillon MJ, Gillin MEA, Ryness JM, De Swiet M. Plasma renin activity and aldosterone concentration in children. *Arch Dis Child*. 1976;51:537-540.

58. Martinez-Aguayo A, Aglony M, Campino C, et al. Aldosterone, plasma renin activity, and aldosterone/renin ratio in a normotensive healthy pediatric population. *Hypertension*. 2010;56:391-396.

59. Nagashima R, O'Reilly RA, Levy G. Kinetics of pharmacologic effects in man: the anticoagulant action of warfarin. *Clin Pharmacol andTherapeutics*. 1969;10:22-35.

60. Compendium.ch. Empressin – summary of product characteristics. Orpha Swiss GmbH. Accessed August 22, 2022. https://compendium.ch/product/1363069-empressin-inf-konz-40-ie-2ml

61. Sottosanti M, Morrison GC, Singh RN, et al. Dehydration in children with diabetic ketoacidosis: a prospective study. *Arch Dis Child*. 2012;97:96-100.

62. Hahn RG. Understanding volume kinetics. *Acta Anaesthesiol Scand*. 2020;64:570-578.

63. Hahn RG. Volume kinetics for infusion fluids. *Anesthesiology*. 2010;113:470-481.

SUPPORTING INFORMATION

Additional supporting information can be found online in the Supporting Information section at the end of this article.